Res Chem Intermed
https://doi.org/10.1007/s11164-018-3334-z

Dicyanomethylene-4*H*-pyran-based NIR fluorescent ratiometric chemosensor for pH measurement

Jinfeng Yang[1,2] · Meng Li[3] · Wei-Hong Zhu[1]

Received: 15 October 2017 / Accepted: 17 February 2018
© Springer Science+Business Media B.V., part of Springer Nature 2018

Abstract A D-π-A featured dicyanomethylene-4*H*-pyran-based dye (DCM-OH) is designed as a pH-sensitive fluorescent chemosensor. In neutral conditions, DCM-OH shows a long absorption wavelength at 431 nm attributed to the DCM chromophore via the intramolecular charge transfer (ICT), but very weak fluorescence around 574 nm. While pH increases from 7.15 to 11.00, DCM-OH shows a bathochromic absorption band at 574 nm due to the increase of the ICT process from the oxygen anion group, shifting the emission band to the NIR region. A DFT calculation has been performed to confirm the ICT enhancement. In this way, an obvious ratiometric fluorescent signal (I_{692}/I_{574}) allows the ratiometric detection of pH, induced by a large Stokes shift of about 118 nm. The fluorescent chemosensor exhibits high sensitivity to H^+ with a pK_a value of 7.21. The strong change in fluorescence intensity with pH allows the determination of pH over a much wider range (typically 7–11). Furthermore, the reversible absorption and fluorescence conversion was also performed with protonation and deprotonation, which makes DCM-OH a simple naked-eye sensitive NIR fluorescent chemosensor for pH measurement.

Electronic supplementary material The online version of this article (https://doi.org/10.1007/s11164-018-3334-z) contains supplementary material, which is available to authorized users.

✉ Wei-Hong Zhu
whzhu@ecust.edu.cn

[1] Shanghai Key Laboratory of Functional Materials Chemistry, School of Chemistry and Molecular Engineering, East China University of Science and Technology, Shanghai 200237, China

[2] College of Chemistry and Chemical Engineering, Key Laboratory for Green Processing of Chemical Engineering of Xinjiang Bingtuan, Shihezi University, Shihezi 832000, China

[3] Department of Environmental Science and Engineering, North China Electric Power University, Baoding 071003, China

Published online: 28 February 2018

Graphical Abstract

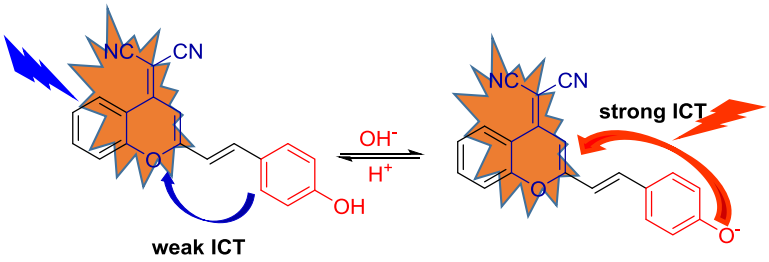

Keywords Fluorescent pH sensor · Dicyanomethylene-4*H*-pyran · Intramolecular charge transfer · Ratiometric response

Introduction

Fluorescent chemosensors have been extensively reported due to their high sensitivity, simplicity and non-invasive imaging [1–4]. It is particularly desirable to develop fluorescent sensors for pH measurement because pH is one of the most important parameters in clinical analysis, pharmacy, industry, the environment and life sciences [5–8]. In fact, the protonation and deprotonation of biomolecules are frequently involved in many cellular events, such as cell growth, cellular proliferation, endocytosis, apoptosis and other processes [9–11]. The detection of pH is extremely significant since intracellular or extracellular pH can reflect severe inflammation and diseases. In addition, pH plays an important role in monitoring food production, freshwater or wastewater treatment procedures and marine sediments [12–15]. Currently, pH fluorescent sensors are widely reported due to their short response time, simple operation, low cost and excellent sensitivity. Intensive efforts have been devoted to pH measurement mainly based on the fluorescence mechanisms of photo-induced electron transfer, intramolecular charge transfer (ICT), and fluorescence resonance energy transfer [16–18]. Most fluorescent chemosensors show turn-off or turn-on behavior [19–21], and some fluorescent chemosensors' emission and absorption are in the ultraviolet–visible (UV–Vis) region. These pH fluorescent chemosensors have disadvantages such as the influences of sensor concentration, instrumental instability and environment interference. Therefore, ratiometric fluorescent sensors are particularly interesting because the ratio of fluorescence intensities at two different wavelengths can eliminate most or all ambiguities [22–24]. However, those sensors with short-wavelength excitation and emission spectra have low signal-to-noise ratios and autofluorescence of biomolecules. Therefore, the ideal ratiometric fluorescent chemosensors are preferable to display a large wavelength shift in the near-infrared (NIR) region [25, 26].

Longer π-electron systems, especially electron donor-π-conjugate–electron acceptor (D-π-A) chromophores, are distinct gateways to design NIR fluorescent

sensors [27–29]. Attributed to its ICT, dicyanomethylene-4*H*-pyran (DCM) is an excellent candidate for NIR fluorophore. Meanwhile, DCM derivatives are very promising due to their broad absorption, long emission wavelength, large Stokes shift, and relatively high fluorescent quantum yield [30, 31]. Thus, DCM-based derivatives, such as NIR fluorescent labels, have been used in various fields including ion recognition [29, 32, 33], logic memory [34, 35], fluorescent molecular switches [36], solar cells [37, 38], fluorescent sensors [39, 40] and in vivo imaging [41–45]. There is a high interest in developing DCM-type ratiometric fluorimetry and lighting up NIR fluorescent chemosensors, and a DCM-OH has been synthesized as shown in Scheme 1, whose optical characters for determining pH have been investigated.

Experimental

Materials and instruments

Toluene, dichloromethane (CH_2Cl_2), chloroform ($CHCl_3$), petroleum ether and acetic acid were purchased from Chinese Chemical Reagent Shanghai Titan Scientific. All solvents were of analytical grade. Nuclear magnetic resonance hydrogen (^1H NMR) and nuclear magnetic resonance carbon (^{13}C NMR) spectra in $CDCl_3$ were measured on a Brucker AV-400 spectrometer (Germany) with tetramethyl silane (TMS) as an internal standard. Ultraviolet–visible (UV–Vis) spectra were obtained by using a Varian Cary 50 spectrophotometer (1 cm quartz cell) at 25 °C. Fluorescence spectra were recorded on a Varian Cary Eclipse fluorescence spectrophotometer (1 cm quartz cell) at 25 °C, and all fluorescence spectra were uncorrected by the photo-multiplier tube response. The width of the slit was 5 nm. TLC analyses were performed on silica gel plates, and column chromatography was conducted over silica gel (mesh 200–300), both of which were obtained from the Qingdao Ocean Chemicals (China).

*1-(2-Hydroxypheny)-1,3-butadione (**1**)*

o-Hydroxyacetophenone (5.0 g, 36.7 mmol) and 30 mL of ethyl acetate were put into a 100-mL rouind-bottom flask. Then, sodium (4.0 g, 170.0 mmol) was added to the flask and the mixture was stirred for 2.5 h at room temperature. After being filtered, the residue was dissolved in water, and the solution was acidified with acetic acid to neutral. After 24 h, compound **1** was obtained in 54% yield.

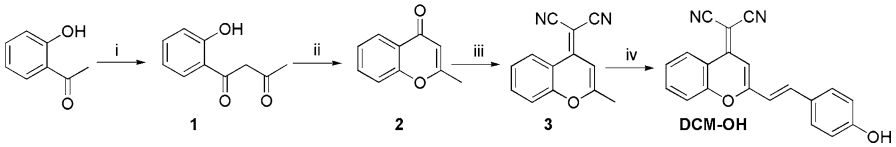

Scheme 1 Synthetic route of DCM-OH: (*i*) $CH_3COOC_2H_5$, Na, 54% yield; (*ii*) HOAc, H_2SO_4, 92% yield; (*iii*) Ac_2O, $CNCH_2CN$, 30% yield; and (*iv*) 4-hydroxybenzaldehyde, piperidine/CH_3CN, 48% yield

*2-Methyl-4-one-4H-chromen (**2**)*

Compound **1** (3.0 g, 16.8 mmol) in acetic acid (30 mL) was refluxed in the presence of 2.0 mL sulfuric acid for 0.5 h. The reaction mixture was poured onto crushed ice, and neutralized with sodium carbonate. The mixture was extracted with dichloromethane. After removing solvents and recrystallized from ethanol, compound **2** was obtained as a gray solid in 92% yield. ^{1}H NMR (400 MHz, $CDCl_3$, ppm): δ 2.39 (s, 3H, –CH_3), 6.18 (s, 1H, –CH =), 7.42 (m, 2H, phenyl-H), 7.64 (d, $J = 8.0$ Hz, 1H, phenyl-H), 8.17 (d, $J = 8.0$ Hz, 1H, phenyl-H).

*4-(Dicyanomethylene)-2-methyl-chromone (**3**)*

Compound **2** (2.0 g, 12.5 mmol) was added to 10.0 mL acetic anhydride of containing malononitrile (1.0 g, 15.1 mmol). After refluxing for 13 h, the mixture was concentrated under reduced pressure. Then, the residue was refluxed for 0.5 h in 30 mL of water. Finally, the solution was filtered to give the crude product, which was recrystallized from ethanol as a gray solid in 30% yield. ^{1}H NMR (400 MHz, $CDCl_3$, ppm): δ 2.45 (s, 3H, –CH_3), 6.73 (s, 1H, –CH =), 7.46 (m, 2H, phenyl-H), 7.73 (m, 1H, phenyl-H), 8.94 (dd, $J_1 = 8.6$, $J_2 = 1.2$ Hz, 1H, phenyl-H).

DCM-OH

Compound **3** (131.2 mg, 0.63 mmol) and 4-hydroxybenzaldehyde (76.9 mg, 0.63 mmol) were taken in 30.0 mL anhydrous toluene under argon, and then piperidine (1.0 mL) and acetic acid (0.5 mL) were added. The contents were refluxed, and monitored by TLC (dichloromethane: petroleum ether). After refluxing for 13 h, the solvent was removed in a rotary evaporator, and the obtained crude product was purified by column chromatography on silica gel with dichloromethane to afford the desired product in 52% yield. ^{1}H NMR (400 MHz, DMSO-d_6): δ 6.85 (d, $J_1 = 8.8$ Hz, 1H), 6.96 (s, 1 H), 7.30 (d, $J = 16.0$ Hz, 1H), 7.59 (m, 3H), 7.70 (d, $J = 16.0$ Hz, 1H), 7.79 (d, $J = 7.6$ Hz,1H), 7.93 (m, 1 H), 8.73 (d, d, $J_1 = 8.4$ Hz, $J_2 = 1.2$ Hz, 1 H), 10.16 (s, 1 H). ^{13}C NMR (100 MHz, $CDCl_3$, ppm): δ = 165.25, 164.14, 158.15, 157.26, 144.51, 140.53, 135.59, 131.33, 129.84, 124.25, 122.65, 122.35, 121.30, 121.15, 110.96, 64.27. HR-MS (*m*/*z*): $[M–H]^+$ Calculated for $C_{20}H_{12}N_2O_2$ 312.0928, found 311.0820.

Results and discussion

Design and synthesis of DCM-OH

As shown in Scheme 1 and Scheme S1 (Supporting Information online), the key intermediate **3** was first obtained by using a condensation reaction of malononitrile and 2-methyl-4-one-4*H*-chromen **2**, which was synthesized from 1-(2-hydroxypheny)-1,3-butadione **1** via Vilsmeier formylation in 92% yield. Then, the D-π-A type pyran derivative DCM-OH was obtained from the reaction of 2-(3,5,5-

trimethylcyclohex-2-enylidene) malononitrile **3** with 4-hydroxybenzaldehyde. Their chemical structures were well characterized by ^{1}H NMR, ^{13}C NMR, and HRMS. In ^{1}H NMR spectra (S1), the characteristic signal at δ 6.96 ppm corresponds to the hydrogen on the pyranyl ring. This is further confirmed by the appearance of a signal at δ 64.3 ppm in the ^{13}C NMR spectra. The presence of a singlet at δ 10.16 ppm in ^{1}H NMR spectrum was attributed to the phenol hydrogen of benzene ring. The presence of (CH=) protons resonance at about δ 7.93 and 7.30 demonstrates the successful synthesis of DCM-OH. Furthermore, the characteristic coupling constant (J = 16.0 Hz) of alkene protons is indicative of the predominant *trans* isomer. These correspond to the appearance of carbon signals in the ^{13}C NMR spectra (S2). The $[M\text{-}H^{+}]^{-}$ peak of HR-MS corresponding to the DCM-O^{-} well supports our proposed mechanism (S3).

Photophysical properties

Figure 1 displays the absorption spectra of DCM-OH (1×10^{-5} M) in several solvents of different polarity. The absorption peak at λ_{max} 450 nm is attributed to the ICT from the 4*H*-pyran in all the solvents. For aprotic polar solvents, such as dimethyl sulfoxide and *N*,*N*-dimethyl formamide (DMF), there are serious disturbances of the solvation effect. In the UV–vis spectra around 650 nm, an absorption band was seen for DMSO and DMF, which might belong to the deprotonated form. And the DMF was unstable in the presence of strong bases such as sodium hydroxide or strong acid such as hydrochloric acid. Moreover, the absorbance decrease with increasing solvent polarity should be attributed to a highly polar-excited state population (ICT) state [46]. Considering the solubility of the DCM-OH in water, the investigation of absorption and emission spectra with pH value in the mixed solvent, C_2H_5OH–H_2O (6:4, v/v), was carried out.

The absorption and emission spectra were measured with varying pH values. Firstly, the solution of free probe DCM-OH shows one major absorption peak at around 450 nm, with another one at about 431 nm. The interaction of pH value for DCM-OH is investigated by means of spectrometric titration experiments using either acid or base. Both the absorption and emission spectra was barely changed

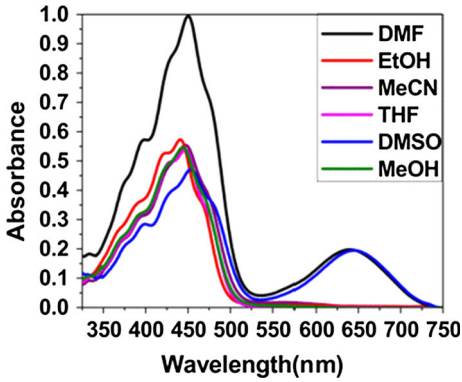

Fig. 1 Absorption spectra of DCM-OH (1.0×10^{-5} M) in different solvents

when $HClO_4$ was added stepwise to the solution of DCM-OH (1×10^{-5} M) at room temperature. However, when NaOH was added stepwise to the solution of DCM-OH, a new absorption peak at λ_{max} 550 nm rose and the absorption peak at λ_{max} 450 nm fell. Obviously, the bathochromic shifted absorption spectra were observed from acidic to basic conditions as shown in Fig. 2.

Next, the fluorescent titration experiments were investigated. There existed a weak emission band at 574 nm upon excitation at isobestic point 494 nm. Simultaneously, a new emission band at 692 nm was enhanced with the increase of pH, during which the fluorescence intensity at 692 nm progressively increased, and the intensity at 574 nm gradually decreased (Fig. 3). Additionally, the maximum emission not only shifted by 118 nm but the color of the solution also changed obviously from yellow to purple with protonation and deprotonation. As a consequence, the ICT-based fluorescent chemosensor DCM–OH can monitor pH in ratiometric applications, specifically as a 'naked-eye' pH sensor.

$$pKa - pH = \log[(A_{max} - A)/(A - A_{min})] \quad (1)$$

As shown in Fig. 4, no absorption spectra change was observed at pH from 3 to 6. At a higher pH, however, the absorbance at 450 nm clearly decreased, along with an increasing broad band at 550 nm. In contrast, upon alkalization from pH 7 to 11, the absorption band of DCM-OH was red-shifted about 100 nm. The plots of absorbance versus pH exhibit S-shaped calibration graphs and the acidity constant pK_a is calculated to be 7.18 by Henderson–Hasselbalch Eq. (1) based on the titration data [7, 17], where A is the observed absorbance at a fixed wavelength, and A_{max} and A_{min} are the maximum and minimal absorbance, respectively.

$$pKa - pH = \log[(F_{max} - F)/(F - F_{min})] \quad (2)$$

The determined pK_a from Eq. 2 was also verified by fitting the individual fluorescence titration curve. The pK_a value of 7.21 was almost in agreement with the data calculated from absorption changes, where F is the observed fluorescent intensity at a fixed wavelength, and F_{max} and F_{min} are the maximum and minimal fluorescent intensity, respectively. As shown in Fig. 5, below pH 7 and above pH 9, the intensity remained almost constant. The fact is that there were no concentration

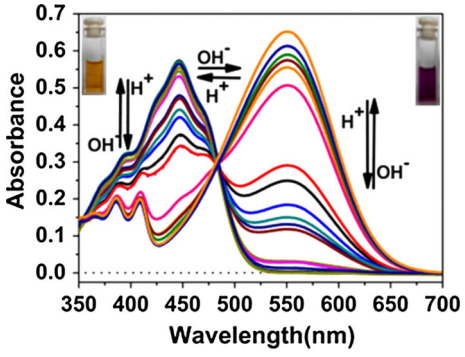

Fig. 2 Changes in absorption spectra of DCM-OH (1.0×10^{-5} M in C_2H_5OH/H_2O, v/v = 6:4) titrated by 0.01 M $HClO_4$ and 0.01 M NaOH in the pH range of 3.08–11.00

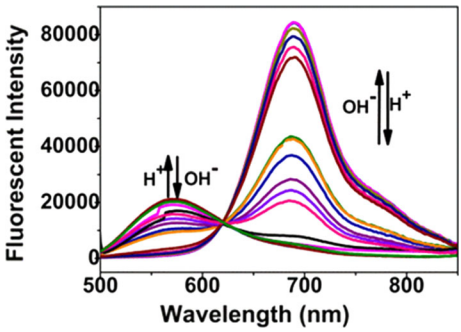

Fig. 3 Changes in fluorescence spectra of DCM-OH (1.0×10^{-5} M in C_2H_5OH/H_2O, v/v = 6:4) titrated by 0.01 M $HClO_4$ and 0.01 M NaOH in the pH range of 3.08–11.00 (excited at the isobestic point of 483 nm)

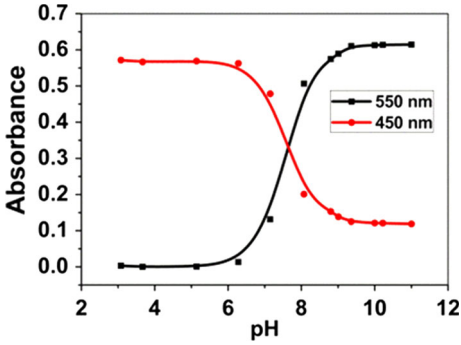

Fig. 4 Plots of absorption (A_{550} and A_{450} are the absorbance at wavelengths of 550 and 450 nm, respectively)

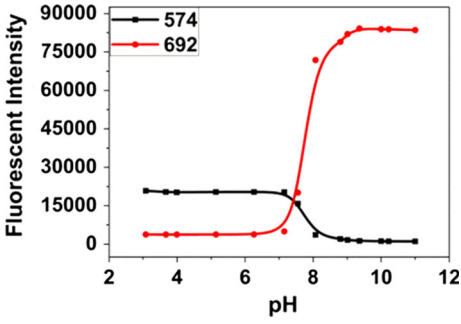

Fig. 5 Plots of emission (I_{692} and I_{574} are the emission intensity at wavelengths of 692 and 574 nm, respectively)

effects in the experiments for that pH range. Moreover, it is obvious that, in the transition range (pH 7–9), there should be a drastic change in the emission intensity. In addition, an obvious ratiometric fluorescent signal (I_{692}/I_{574}) is observed (Fig. 6) which provides us with another way to monitor pH. Upon deprotonation, the fluorescence intensity enhancement ($FE = I_{692}/I_{574}$) is calculated by the emission maximum at 692 nm to that at 574 nm. The ratio of I_{692}/I_{574} recorded in the examined pH interval (from 8 to 11) is more than 20 times and the maximum FE is 79. From acidification to alkaline media, the maximum emission shift is about 118 nm. The Stokes shift remained almost constant above pH 8. Correspondingly, the solution changes obviously from yellow to purple. Figure 7 shows absorption

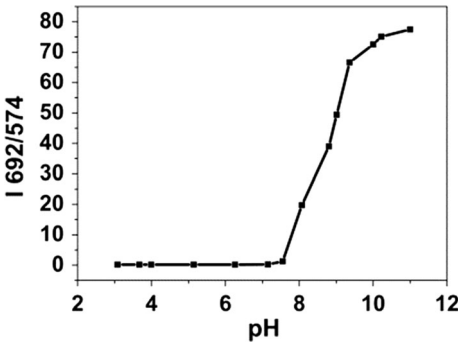

Fig. 6 The ratio of the fluorescence intensity at 692 nm to that at 574 nm with various pH

Fig. 7 **a** The color changes of DCM-OH (1.0×10^{-5} M in C_2H_5OH/H_2O, v/v = 6:4) titrated by 0.01 M $HClO_4$ and 0.01 M NaOH in the pH range of 3.08–11.00. **b** Visible color changes of DCM-OH by indicator paper dipping into 0.01 M $HClO_4$ (*a*) and 0.01 M NaOH solution (*b*) for 3 min

photographs of DCM-OH with protonation and deprotonation. These results indicate that the dye DCM-OH is an excellent ratiometric fluorescent chemosensor [47, 48], and also a "naked-eye" NIR probe for determining pH changes. However, the system is operable in $EtOH/H_2O$ (60/40 v/v), and such a high level of organic solvent could weaken the system in practical applications.

It is known that DCM moiety, with a typical D-π-A system, possesses an excellent ICT effect. Initially, DCM-OH possesses an ICT structure with absorption at λ_{max} 450 nm and emission spectra at λ_{max} 574 nm. The alkali state is a "push–pull" π electron system with the oxygen anion as a stronger donor than the phenolic group, and DCM as an acceptor. Deprotonation creates a stronger phenolate donor, and DCM-OH exhibits an absorption band at λ_{max} 550 nm and an emission band at λ_{max} 692 nm along with a strong fluorescent intensity. The remarkable changes in both absorption and fluorescence spectra should be mainly attributed to the intensive ICT process resulting from a stronger efficient electron-push capacity of the oxygen anion (Fig. 8). Moreover, the structural change is taking place in the pH range of 7–8. Furthermore, the fluorescent intensity at λ_{max} 692 nm increases to the maximum within 3 min and then stays stable during the testing time. As a result, the fluorescence can be repeatedly modulated by pH.

Finally, the HOMO and LUMO frontier orbitals of DCM-OH are shown in Fig. 9. With the DFT calculation, the separation energy ($\Delta\varepsilon = \varepsilon_{LUMO} - \varepsilon_{HOMO}$) is 5.05 eV. It is obvious that the orbit modeling of DCM-OH is the '*trans*-' configuration. The conjugation is clearly predicted by the calculations of HOMO, since the electron density is mainly centered at the conjugated system by benzene

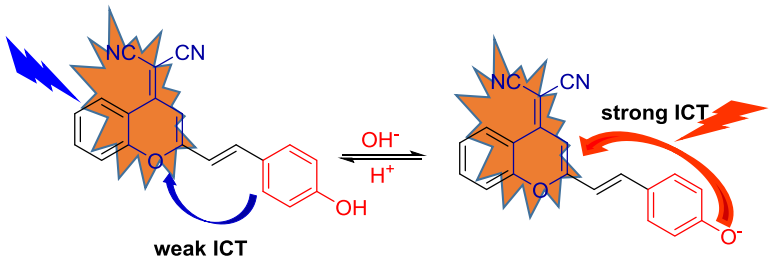

Fig. 8 Conversion mechanism of DCM-OH

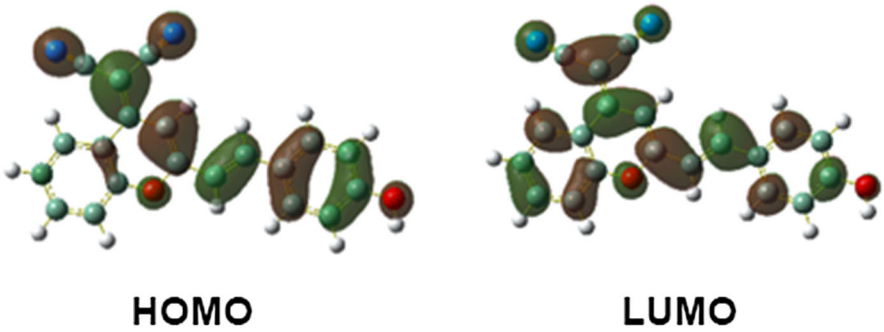

Fig. 9 Frontier molecular orbitals of DCM-OH

antenna. The LUMO, as expected, spread over the whole molecule backbone including the benzene moiety.

Conclusions

We have developed a ratiometric NIR fluorescent chemosensor for determining pH changes over a wide pH scale. The large Stokes shift from both absorption and emission spectra makes DCM-OH available to the NIR region. The proposed strategy by modulation of pH via protonation or deprotonation provides a promising methodology for design of ratiometric fluorimetry. Furthermore, DCM-OH displays a color change from yellow to purple upon the addition of OH^-, which can serve as a "naked-eye" chemosensor. Meanwhile, for the D-π-A featured DCM-OH, the deprotonation can increase the ICT process comntributing to a stronger electron-push capacity of the oxygen anion than the phenolic hydroxyl group. Correspondingly, the DFT calculation demonstrates that a stronger ICT process from DCM-O^- is possuible. As demonstrated, DCM-OH is a promising colorimetric pH sensitive chemosensor in the NIR region.

Acknowledgements This work was supported by Natural Science Foundation of China (21788102, and 21607044), and Natural Science Foundation of Hebei Province (B2017502069).

References

1. S.Y. Chen, M. Zhao, J. Su, Q. Zhang, X.H. Tian, S.L. Li, H.P. Zhou, J.Y. Wu, Y.P. Tian, Dyes Pigments **136**, 807 (2017)
2. E. Poehler, S.A. Pfeiffer, M. Herm, M. Gaebler, B. Busse, S. Nagl, Anal. Bioanal. Chem. **408**, 2927 (2016)
3. H.N. Kim, E.-H. Lee, Z.C. Xu, H.-E. Kim, H.-S. Lee, J.-H. Lee, J. Yoon, Biomaterials **33**, 2282 (2012)
4. X.J. Jiang, Y. Fu, H. Tang, S.Q. Zang, H.W. Hou, T.C.W. Mak, H.Y. Zhang, Sens. Actuators B **190**, 844 (2014)
5. Y.Q. Tian, F.Y. Su, W. Weber, V. Nandakumar, B.R. Shumwar, Y.G. Jin, X.F. Zhou, M.R. Holl, R.H. Johnson, D.R. Meldrum, Biomaterials **31**, 7411 (2010)
6. N.I. Georgiev, R. Bryaskova, R. Tzoneva, I. Ugrinova, C. Detrembleur, S. Miloshev, A.M. Asiri, A.H. Qusti, V.B. Bojinov, Bioorg. Med. Chem. **21**, 6292 (2013)
7. K. Makhal, D. Goswami, J. Fluoresc. **27**, 339 (2017)
8. X.F. Zhou, F.Y. Su, H.G. Lu, P. Senecal-willis, Y.Q. Tian, R.H. Johnson, D.R. Meldrum, Biomaterials **33**, 71 (2012)
9. R.C. Adochite, A. Moshnikova, J. Golijanin, O.A. Andreev, N.V. Katenka, Y.K. Reshetnyak, Mol. Imaging Biol. **18**, 686 (2016)
10. L.A. Yan, H. Shi, D.G. He, X.X. He, K.M. Wang, F.Z. Xu, Sci. China Chem. **59**, 802 (2016)
11. C. Demuth, J. Varonier, V. Jossen, R. Eibl, D. Eibl, Appl. Microbiol. Biotechnol. **100**, 3853 (2016)
12. S. Chang, X.M. Wu, Y.S. Li, D.C. Niu, Y.P. Gao, Z. Ma, J.L. Gu, W.R. Zhao, W.H. Zhu, Biomaterials **34**, 10182 (2013)
13. X.X. Zhang, Z. Wang, X.Y. Yue, Y. Ma, D.O. Kiesewetter, X.Y. Chen, Mol. Pharm. **10**, 1910 (2013)
14. Y. Li, H.Y. Yang, D.S. Lee, Pharm. Res. **33**, 2358 (2016)
15. M.F. Chung, H.Y. Liu, K.J. Lin, W.T. Chia, H.W. Sung, Angew. Chem. Int. Ed. **54**, 1 (2015)
16. N.I. Georgiev, A.M. Asiri, A.H. Qusti, K.A. Alamry, V.B. Bojinov, Dyes Pigments **102**, 35 (2014)
17. C.M. Sha, Y.H. Chen, Y.F. Chen, D.M. Xu, J. Fluoresc. **26**, 1709 (2016)
18. M.H. Lee, J. Fluoresc. **26**, 807 (2016)
19. Z.H. Pan, G.G. Luo, J.W. Zhou, J.X. Xia, K. Fanf, R.B. Wu, Dalton. Trans. **43**, 8499 (2014)
20. Y. Xu, Z. Jiang, Y. Xiao, F.Z. Bi, J.Y. Miao, B.X. Zhao, Anal. Chim. Acta **820**, 146 (2014)
21. K. Karaoglu, F. Yilmaz, E. Mentese, J. Fluoresc. **27**, 1293 (2017)
22. J.T. Hutt, J. Jo, A. Olasz, C.H. Chen, D. Lee, Z.D. Aron, Org. Lett. **14**, 3162 (2012)
23. F.H. Liang, D. Wang, P.Y. Ma, X.H. Wang, D.Q. Song, Y. Yu, Chem. Res. Chin. Univ. **31**, 724 (2015)
24. Y. Zhou, J.F. Zhang, J. Yoon, Chem. Rev. **114**, 5511 (2014)
25. B.C. Zhu, H. Kan, J.K. Liu, H.Q. Liu, Q. Wei, B. Du, Biosens. Bioelectron. **52**, 298 (2014)
26. Z.Q. Guo, S.W. Nam, S. Park, J. Yoon, Chem. Sci. **3**, 2760 (2012)
27. L.N. Wang, M. Liang, Y. Zhang, F.Y. Cheng, X.D. Wang, Z. Sun, S. Xue, Dyes Pigments **101**, 270 (2014)
28. X.M. Wu, S. Chang, X.R. Sun, Z.Q. Guo, Y.S. Li, J.B. Tang, Y.Q. Shen, J.L. Shi, H. Tian, W.H. Zhu, Chem. Sci. **4**, 1221 (2013)
29. Z.D. Tian, Y.C. Liu, B.Z. Tian, J.L. Zhang, Res. Chem. Intermed. **41**, 525 (2015)
30. Z. Guo, W.H. Zhu, M.M. Zhu, X.M. Wu, H. Tian, Chem. Eur. J. **16**, 14424 (2010)
31. Y. Cheng, B.Y. Zhu, Y. Deng, Z.R. Zhang, Anal. Chem. **87**, 4781 (2015)
32. J. Cao, C.C. Zhao, W.H. Zhu, Chem. Commun. **48**, 6073 (2012)
33. W.H. Zhu, X.M. Huang, Z.Q. Guo, X.M. Wu, H.H. Yu, H. Tian, Chem. Commun. **48**, 1784 (2012)
34. Z.Q. Guo, P. Zhao, W.H. Zhu, X.M. Huang, Y.S. Xie, H. Tian, J. Phys. Chem. C **112**, 7047 (2008)
35. Z.Q. Guo, W.H. Zhu, L.J. Shen, H. Tian, Angew. Chem. Int. Ed. **46**, 5549 (2007)
36. J.F. Yang, M. Li, L.H. Kang, W.H. Zhu, Sci. China Chem. **60**, 607 (2017)
37. S. Franco, J. Garin, N.M. de Baroja, R. Pérez-Tejada, J. Orduan, Y.H. Yu, M. Lira-Cantú, Org. Lett. **14**, 752 (2012)
38. Z.Q. Guo, W.H. Zhu, H. Tian, Chem. Commun. **48**, 6073 (2012)
39. L.J. Shen, X.Y. Lu, H. Tian, W.H. Zhu, Macromolecules **44**, 5612 (2011)
40. M. Li, X.M. Wu, Y. Wang, Y.S. Li, W.H. Zhu, T.D. James, Chem. Commun. **50**, 1751 (2014)
41. K.Z. Gu, Y.S. Xu, H. Li, Z.Q. Guo, S.J. Zhu, S.Q. Zhu, P. Shi, J. Am. Chem. Soc. **138**, 5334 (2016)

42. X.M. Wu, X.R. Sun, Z.Q. Guo, J.B. Tang, Y.Q. Shen, T.D. James, H. Tian, W.H. Zhu, J. Am. Chem. Soc. **136**, 3579 (2014)
43. Y. Cheng, B.Y. Zhu, X. Li, G.B. Li, S.Y. Yang, Z.R. Zhang, Bioorg. Med. Chem. Lett. **25**, 4472 (2015)
44. J.H. Ma, J.L. Fan, H.D. Li, Q.C. Yao, J. Xia, J.Y. Wang, X.J. Peng, Dyes Pigments **138**, 39 (2017)
45. J.F. Wang, B. Li, W.Y. Zhao, X.F. Zhang, X. Luo, M.E. Corkins, S.L. Cole, C. Wang, Y. Xiao, X.M. Bi, Y. Pang, C.A. McElroy, A.J. Bird, Y.Z. Dong, ACS Sens. **1**, 882 (2016)
46. S.A. El-Daly, K.A. Alamry, J. Fluoresc. **26**, 163 (2016)
47. K.X. Xiang, S.Z. Chang, J.J. Feng, C.J. Li, W. Ming, Z.Y. Liu, Y.C. Liu, B.Z. Tian, J.L. Zhang, Dyes Pigments **134**, 190 (2016)
48. K.X. Xiang, Y.C. Liu, C.J. Li, B.Z. Tian, T.Z. Tong, J.L. Zhang, Dyes Pigments **123**, 78 (2015)